Journal of Theoretical Medicine, Vol. 1, pp. 223-235
Reprints available directly from the publisher
Photocopying permitted by license only

Necrosis and Apoptosis: Distinct Cell Loss Mechanisms in a Mathematical Model of Avascular Tumour Growth

H. M. BYRNE[a,*] and M. A. J. CHAPLAIN[b,†]

[a]*Department of Mathematics, UMIST, PO BOX 88, Manchester M60 1QD, U.K.;* [b]*Department of Mathematics and Computer Science, University of Dundee, Dundee DD1 4HN*

(Received 11 March 1997; In final form 9 June 1997)

During the initial avascular phase of solid tumour growth, it is the balance between cell proliferation and cell loss that determines whether the tumour colony expands or regresses. Experimentalists have identified two distinct mechanisms that contribute to cell loss. These are apoptosis and necrosis. Cell loss due to apoptosis may be referred to as programmed-cell-death, occurring, for example, when a cell exceeds its natural lifespan. In contrast, cell loss due to necrosis is induced by changes in the cell's microenvironment, occurring, for example, in nutrient-depleted regions of the tumour.

In this paper we present a mathematical model that describes the growth of an avascular tumour which comprises a central core of necrotic cells, surrounded by an outer annulus of proliferating cells. The model distinguishes between apoptosis and necrosis. Using a combination of numerical and analytical techniques we present results which suggest how the relative importance of apoptosis and necrosis changes as the tumour develops. The implications of these results are discussed briefly.

Keywords: Cell loss, Avascular tumour, apoptosis, micronenvironment

1 INTRODUCTION

In vivo cancer growth is a complex phenomenon, involving many inter-related processes and consequently the mathematical modelling of such processes is very difficult. Broadly speaking, solid tumour growth can be divided into two distinct stages: the avascular and the vascular phases. Bridging these phases is a process called angiogenesis by which the tumour elicits a new blood supply from neighbouring blood vessels (Folkman, 1976; Muthukkaruppan, 1982). The relatively harmless avascular growth phase, which we discuss below, corresponds to diffusion-limited growth, with cells receiving vital nutrients and disposing of waste products via diffusion processes across the outer boundary of the tumour. By contrast, once vascularised, the tumour's nutrient supply is effectively limitless and rapid, potentially lethal growth ensues.

Whilst several models have been developed to describe angiogenesis and vascular tumour growth (Balding and McElwain, 1985; Chaplain and Stuart,

*Corresponding Author: E-mail: h.byrne@umist.ac.uk.
†E-mail: chaplain@mcs.dundee.ac.uk.

1993; Chaplain, 1995; Byrne and Chaplain, 1995b; Orme and Chaplain, 1996), over the past twenty years most of the mathematical models appearing in the literature have focussed on solid tumour growth (Adam, 1986; Byrne and Chaplain, 1995a, 1996a, b; Durand, 1990; Greenspan, 1972; Landry *et al.*, 1982; McElwain and Morris, 1978; Mueller-Klieser, 1987; Ward and King, 1997). This focus of interest has been guided largely by the relative abundance of *in vitro* studies involving multicellular spheroids (MCS) (Sutherland and Durand, 1984; Freyer *et al.*, 1984; Groebe and Mueller-Klieser, 1991, 1996; Kerr, 1971; Kerr *et al.*, 1972; Kerr *et al.*, 1994). MCS are widely used in the laboratory because the well-defined and reproducible manner in which they grow mimics the earliest phase of *in vivo* avascular tumour growth. Thus, in addition to providing insight into the structure and division of tumour cells, MCS can be used to provide some indication of a tumour's handling of a proposed chemical or drug *in vivo* (Hiltman and Lory, 1983).

Typically, mathematical models of MCS treat the tumour as a spherical mass of cells which grows in response to an external nutrient supply. It is assumed that the internal architecture consists of a central necrotic core surrounded by a layer of proliferating cells — a third, intermediate region containing non-proliferating, quiescent cells is also sometimes included. Many of the existing deterministic models comprise an ordinary differential equation (ODE) and at least one reaction-diffusion equation (RDE) (Adam, 1986; Greenspan, 1972). The ODE derives from mass conservation applied to the tumour and describes the evolution of the tumour boundary whereas the RDEs describe the distribution within the tumour of nutrients such as oxygen and glucose and growth inhibitory factors such as chalones. Any interior boundaries, such as the interface between the necrotic core and the quiescent region, are defined implicitly, occurring, for example, when the nutrient concentration attains a prescribed value. Analysis of such models enables the relative importance of the different mechanisms involved in the growth process to be examined.

Clearly the growth rate of the tumour is determined by the balance between cell proliferation and cell loss. The nutrient provides the energy needed to maintain the tumour cells and also for cell division. Experimental results suggest that two mechanisms contribute to cell loss: apoptosis and necrosis (Kerr, 1971; Kerr *et al.*, 1972; Kerr *et al.*, 1994). Cell loss due to apoptosis is *natural*, or programmed, cell death whereas cell loss due to necrosis is *unnatural* and induced by changes in the cell's microenvironment. Whilst there is some ambiguity in the literature regarding the precise difference between apoptosis and necrosis, here we define it as follows. Necrosis is induced by the external microenvironment whereas apoptosis is an intrinsic property of a cell. Thus, the low nutrient levels found towards the centre of a tumour may trigger cell death due to necrosis whilst if a cell lives beyond its natural lifespan then cell death due to apoptosis may occur. More recently, *in situ* labelling techniques led Kressel and Groscurth (1994) to make the following distinction between apoptosis and necrosis. Cells undergoing apoptosis are characterised by DNA fragmentation that follows a well-defined sequence which is initiated when the cell starts to die. By contrast, cells undergoing necrosis show no signs of DNA fragmentation until 24 hours after the onset of necrosis.

Recent experimental results highlight the significance of apoptosis in tumour development (Kastan *et al.*, 1995; Merritt *et al.*, 1995; Potten, 1992; Watson *et al.*, 1996). For example, Thames *et al.* (1996) have shown that downregulation of apoptosis is responsible for the rapid growth of murine-ovarian carcinoma and Shao *et al.* (1996) have correlated low apoptotic indices with poor clinical prognosis in human breast cancer. Genetic mutations in the tumour cells may be responsible for the observed changes in apoptosis. Indeed, it is now known that mutations in the tumour suppressor gene p53 can lead to a reduction in cell death due to apoptosis. Other genetic alterations that lead to overexpression of the proto-oncogene bcl-2 have also been implicated in the development of a range of cancers, including non-Hodgkins

lymphoma (Kiberu *et al.*, 1996), prostate cancer (Tu *et al.*, 1996) and colorectal neoplasia (Hawkins *et al.*, 1997). The functions of bcl-2 are manifold. For example, bcl-2 is known to inhibit both apoptosis and necrosis (Kane *et al.*, 1997). The interplay between apoptosis and necrosis has been studied by Eerola *et al.* (1997) who showed that apoptosis is inversely related to the extent of necrosis in small cell lung carcinoma. In the light of such experimental results, it is timely to consider the effect that both necrosis and apoptosis have on tumour growth.

Necrotic cell loss has been incorporated into most models of MCS growth (Adam, 1986; Greenspan, 1972) whereas apoptotic cell loss has been largely neglected. It is possible to show that, when apoptosis is neglected, these models cannot support steady, time-independent tumour configurations which comprise only proliferating cells — a situation which can arise in practice (Tubiana, 1971). In this, paper we incorporate apoptosis into our mathematical model and show how its inclusion is crucial to realising steady, nonnecrotic tumours. To our knowledge, to date, apart from (Byrne and Chaplain, 1995a, 1996a), only (McElwain and Morris, 1978) have incorporated apoptosis into a spatio-temporal mathematical model of solid tumour growth. Under certain conditions, the model of McElwain and Morris (1978) admits steady solutions which do not possess a necrotic core: the steady state tumour comprises a central core, in which the rates of nutrient consumption and cell proliferation fall, surrounded by an outer, proliferating rim.

In this paper we use a combination of numerical and analytical techniques to study the manner in which the relative importance of apoptosis and necrosis as distinct cell loss mechanisms changes as the tumour develops. At the same time we try to indicate the key similarities and differences between the approach adopted here and that used by other authors. In this sense, the paper may be viewed as a summary of existing work, with the emphasis placed on interpretation of the main results in a way which is accessible to mathematicians and biologists alike.

2 A PRELIMINARY MODEL OF AVASCULAR TUMOUR GROWTH

The mathematical model presented below describes the evolution of a multicellular spheroid growing in response to an externally-supplied nutrient such as oxygen or glucose. We assume that the tumour is radially-symmetric and contains proliferating and necrotic cells, the proportion of each cell type changing as the tumour grows. We denote by $R(t)$ the outer radius of the tumour and by $r_{\text{nec}}(t)$ its necrotic radius, so that if the tumour comprises proliferating cells alone then $r_{\text{nec}} = 0$.

The model consists of an RDE which describes the distribution of the nutrient (σ) and an integro-differential equation which governs the evolution of $R(t)$. The necrotic radius r_{nec} is defined implicitly, occurring where σ attains a specified value (σ_{nec}) and such that cell proliferation is possible only in nutrient-rich regions where $\sigma > \sigma_{\text{nec}}$ and necrosis occurs in nutrient-depleted regions where $\sigma < \sigma_{\text{nec}}$. Fuller derivations of the mathematical model can be found in (Byrne and Chaplain, 1995a, 1996a, b). Here, for brevity, the governing equations are presented in dimensionless form in spherical polar coordinates with radial symmetry.

$$0 = \frac{1}{r^2}\frac{\partial}{\partial r}\left(r^2\frac{\partial \sigma}{\partial r}\right) - \Gamma H(r - r_{\text{nec}}), \quad (2.1)$$

$$R^2\frac{dR}{dt} = \int_0^R \{S(\sigma)H(r - r_{\text{nec}}) - N(\sigma) \times H(r_{\text{nec}} - r)\}r^2 dr, \quad (2.2)$$

subject to

$$\frac{\partial \sigma}{\partial r} = 0 \text{ on } r = 0, \quad (2.3)$$

$$\sigma = \sigma_\infty \text{ on } r = R(t), \quad (2.4)$$

$$\sigma, \frac{\partial \sigma}{\partial r} \text{ continuous across } r = r_{\text{nec}}, \quad (2.5)$$

$$\sigma(r_{\text{nec}}, t) = \sigma_{\text{nec}}, \quad (2.6)$$

$$R(t = 0) = R_0. \quad (2.7)$$

In (2.1) we have adopted the usual quasi-steady approach, with $\partial\sigma/\partial t = 0$. This approximation

occurs because a typical nutrient diffusion timescale is much shorter than a typical tumour doubling timescale (Adam, 1986; Adam and Maggelakis, 1990; Chaplain and Britton, 1993; Chaplain *et al.*, 1994; Greenspan, 1972). Since the necrotic core contains only dead cells we assume that any nutrient consumption terms vanish there. Thus, denoting by $H(\cdot)$ the Heaviside step-function ($H(x) = 1$ if $x > 0, H(x) = 0$ if $x \leq 0$), the term $\Gamma H(r - r_{\text{nec}})$ describes nutrient consumption by the proliferating cells, which we assume occurs at the constant rate Γ.

In (2.2) we introduce $S(\sigma)$ and $N(\sigma)$ to denote cell proliferation and cell loss due to necrosis respectively. We assume that cell proliferation is confined to the annulus $r_{\text{nec}} < r < R$ and that it represents a balance between cell birth, or mitosis, and apoptosis. Necrotic cell loss is restricted to nutrient-depleted regions of the tumour where $\sigma < \sigma_{\text{nec}}$. Following (Byrne and Chaplain, 1995a, 1996a), and to simplify the analysis, throughout this paper attention is focussed on a proliferation rate which is linear with respect to σ. Thus we propose

$$S(\sigma) = s(\sigma - \tilde{\sigma}),$$

where s and $\tilde{\sigma}$ are positive constants. We interpret $s\sigma$ as the cell proliferation rate and $s\tilde{\sigma}$ as the apoptotic cell loss rate. Assuming further that necrosis manifests itself as a constant volume loss term at all points inside the necrotic core, we fix

$$N(\sigma) = 3s\lambda H(r - r_{\text{nec}}).$$

We remark that experimentally determined functions could be used to describe $S(\sigma), N(\sigma)$ and the nutrient consumption term (Freyer *et al.*, 1984; Groebe and Mueller-Klieser, 1996; Hiltman and Lory, 1983; Landry *et al.*, 1982). Since such models are usually only amenable to numerical solution, here we restrict attention to simpler expressions in order to focus on the methodology of our approach.

Substituting with $S(\sigma)$ and $N(\sigma)$, equation (2.2) can be rewritten thus:

$$R^2 \frac{dR}{dt} = s \int_{r_{\text{nec}}}^{R} (\sigma - \tilde{\sigma}) r^2 dr - s\lambda r_{\text{nec}}^3. \tag{2.8}$$

Equations (2.3)–(2.7) close equations (2.1) and (2.8). Equation (2.3) reflects the assumed symmetry of the tumour. In (2.4) σ_∞ is the constant nutrient concentration exterior to the tumour and, by continuity, on its outer tumour boundary. (2.5) ensures continuity of σ and $\partial\sigma/\partial r$ across the necrotic boundary whilst (2.6) defines r_{nec} implicitly. Finally, (2.7) defines the initial, scaled tumour radius.

3 MODEL SIMPLIFICATION AND ANALYSIS

Integrating (2.1) subject to (2.3)–(2.6) yields an expression for the nutrient concentration within the tumour and also an identity defining $r_{\text{nec}}(t)$ in terms of $R(t)$:

$$\sigma(r, t) = \begin{cases} \sigma_{\text{nec}} \\ \quad \text{for } r \in [0, r_{\text{nec}}), \\ \sigma_{\text{nec}} - \dfrac{\Gamma r_{\text{nec}}^2}{2} + \dfrac{\Gamma r^2}{6} + \dfrac{\Gamma r_{\text{nec}}^3}{3r}, \\ \quad \text{for } r \in [r_{\text{nec}}, R], \end{cases}$$

$$\sigma_\infty - \tilde{\sigma} = \frac{\Gamma R^2}{6}\left(1 + \frac{2r_{\text{nec}}^2}{R^3} - \frac{3r_{\text{nec}}^2}{R^2}\right). \tag{3.1}$$

Substitution with σ in (2.8) then yields the following equation for $R(t)$:

$$\frac{R^2}{s}\frac{dR}{dt} = \frac{(\sigma_{\text{nec}} - \tilde{\sigma})}{3}(R^3 - r_{\text{nec}}^3) - \lambda r_{\text{nec}}^3 + \frac{\Gamma}{6}\left\{\frac{1}{5}(R^5 - r_{\text{nec}}^5) - R^2 r_{\text{nec}}^2 (R - r_{\text{nec}})\right\}. \tag{3.2}$$

Thus the model reduces to (3.2), a nonlinear ODE describing the evolution of $R(t)$, and (3.1), an algebraic identity that relates $r_{\text{nec}}(t)$ to $R(t)$.

It is possible to show that if the tumour comprises proliferating cells only ($r_{\text{nec}} = 0$) then the above expressions for σ and R simplify to give:

$$\sigma(r, t) = \sigma_\infty - \frac{\Gamma}{6}(R^2 - r^2), \tag{3.3}$$

$$\frac{1}{s}\frac{dR}{dt} = \frac{R}{3}\left(\sigma_\infty - \tilde{\sigma} - \frac{\Gamma R^2}{15}\right). \tag{3.4}$$

From (3.3) we see that the minimum nutrient concentration occurs at $r = 0$, and that this minimum value decreases as R increases. Provided that $\sigma(0, t) > \sigma_{\text{nec}}$ the tumour remains a uniform mass of proliferating cells. Fixing $\sigma(0, t) = \sigma_{\text{nec}}$ and rearranging (3.3) we are able to make the following prediction:

- *Necrosis is initiated when the tumour radius passes through a critical value R^* which is defined in terms of the underlying system parameters as follows:* $R^* = [6(\sigma_\infty - \sigma_{\text{nec}})/\Gamma]^{1/2}$.

By varying the external nutrient concentration σ_∞ and measuring the tumour radius at which necrosis is first detected in an MCS, it should be possible to use this result to validate this model prediction by comparing the experimental and predicted values of R^*. The result could also be used for parameter estimation. For example, if σ_∞ and σ_{nec} are known and R^* is measured at the onset of necrosis then we can estimate the rate at which the tumour cells consume the nutrient using $\Gamma = 6(\sigma_\infty - \sigma_{\text{nec}})/R^{*2}$. Equally, if σ_∞ and Γ are known and R^* is measured experimentally, we can predict the nutrient concentration at the onset of necrosis.

From (3.3) and (3.4) we note that when $R = R^*$

$$\frac{dR}{dt} = \frac{s}{15R^*}(3\sigma_\infty - 5\tilde{\sigma} + 2\sigma_{\text{nec}}) \equiv \Lambda, \text{ say.} \quad (3.5)$$

Thus, if $\Lambda > 0$ then the tumour continues to grow and the necrotic core persists. Otherwise, if $\Lambda < 0$ then the tumour shrinks and the necrotic core disappears.

More generally, numerical simulations of the model equations suggest that the tumour will ultimately (as $t \to \infty$) adopt one of three configurations. In the first case the limiting configuration possesses an interior necrotic core. In the second case there is no necrotic core ($r_{\text{nec}} = 0$). In the third case, the tumour disappears. Typical examples of each type of behaviour are presented in Figures 1 to 3. These simulations show how the limiting behaviour depends upon the relative importance of cell loss due to apoptosis, cell proliferation and cell loss due to necrosis, as embodied in the parameters $\tilde{\sigma}$, σ_∞ and σ_{nec} respectively. Indeed as $\tilde{\sigma}$ decreases decay of the tumour to zero (Figure 3) is superceded first by evolution of the tumour to a steady, nonnecrotic configuration for moderate values of $\tilde{\sigma}$ (Figure 2) and then to a steady necrotic configuration for even smaller values of $\tilde{\sigma}$ (Figure 3). As mentioned in the introduction, such a decrease in $\tilde{\sigma}$ may be a consequence of a mutation which diminishes the ability of the gene p53 to trigger apoptosis (Merritt *et al.*, 1995; Potten, 1992; Watson *et al.*, 1996).

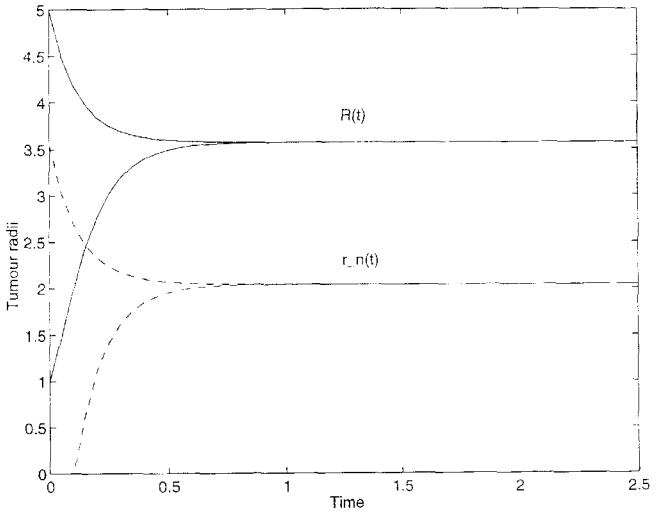

FIGURE 1 Evolution of R and r_{nec} showing how, for a particular set of parameter values, all initial data converge to the limiting values $R \sim 2.42$ and $r_{\text{nec}} \sim 0.63$. Parameter values: $\sigma_\infty = 0.8.\sigma_{\text{nec}} = 0.4$, $\tilde{\sigma} = 0.5$, $\lambda = 0.1$, $\Gamma = 25$, $s = 100$.

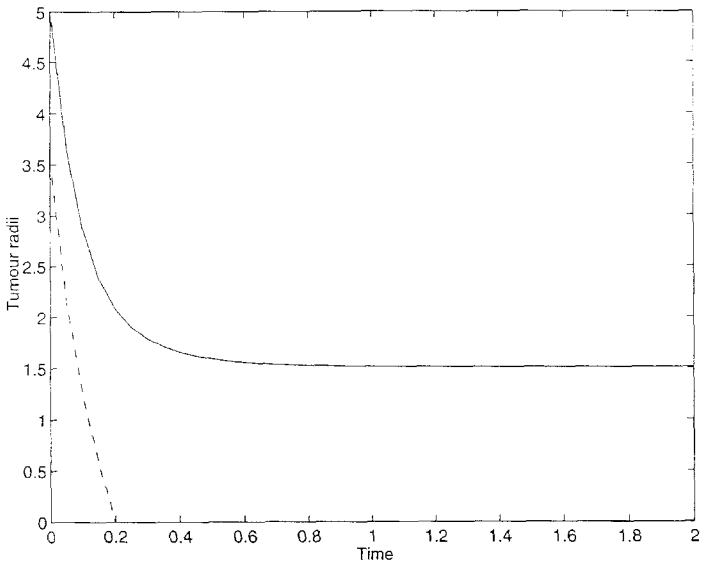

FIGURE 2 Evolution of R and r_{nec} when the rate of cell loss due to apoptosis is increased from $\tilde{\sigma} = 0.5$ (Figure 1) to $\tilde{\sigma} = 0.7$. All initial data converge to a nonnecrotic tumour for which $R \sim 1.51$ and $r_{\text{nec}} = 0.0$. Parameter values: $\sigma_\infty = 0.8.\sigma_{\text{nec}} = 0.4, \tilde{\sigma} = 0.7, \lambda = 0.1, \Gamma = 25, s = 100$.

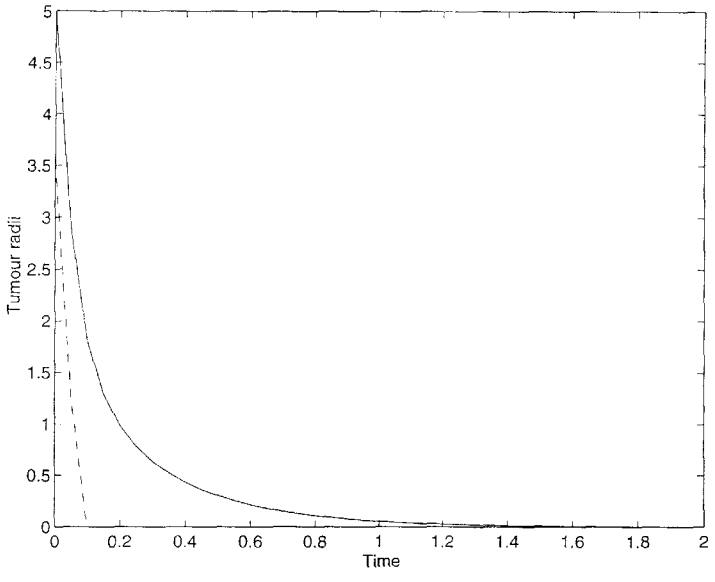

FIGURE 3 Evolution of R and r_{nec} when the rate of cell loss due to apoptosis is increased to $\tilde{\sigma} = 0.9$. All initial data converge to the trivial solution for which $R = 0 = r_{\text{nec}}$. Parameter values: $\sigma_\infty = 0.8.\sigma_{\text{nec}} = 0.4, \tilde{\sigma} = 0.9, \lambda = 0.1, \Gamma = 25, s = 100$.

When $dR/dt = 0$ in (3.2) the model reduces to two coupled equations which define the steady or limiting tumour configurations in terms of the system parameters. In Figure 4 we show how these steady state solutions depend on $\tilde{\sigma}$, the rate of cell loss due to apoptosis. From this diagram we note that the trivial, tumour-free solution ($R = 0 = r_{\text{nec}}$) persists for all parameter values and that nontrivial solutions exist only when $\tilde{\sigma} < \sigma_\infty$. We remark further that where they exist the nontrivial solutions are unique so that only one tumour configuration can be realised.

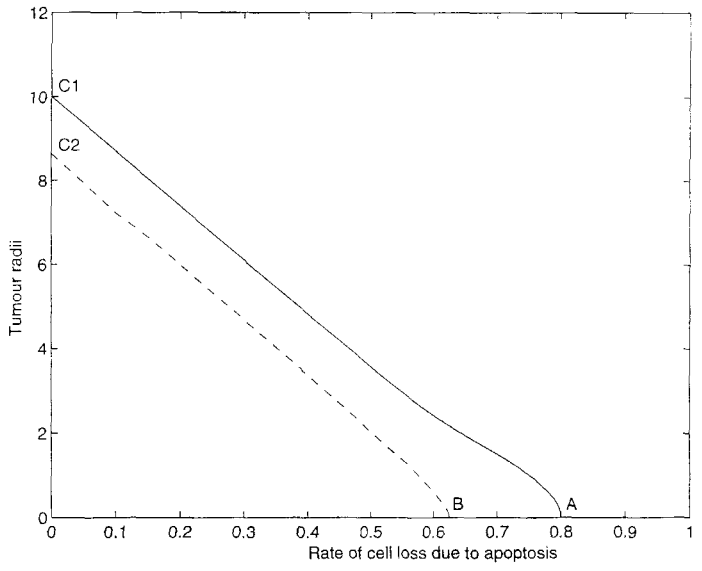

FIGURE 4 Dependence of the steady state tumour radii R and r_{nec} on the rate of cell loss due to apoptosis, $\tilde{\sigma}$. The existence of necrotic and nonnecrotic tumours is restricted to a finite range of $\tilde{\sigma}$. Parameter values: $\sigma_\infty = 0.8.\sigma_{\text{nec}} = 0.4$, $\lambda = 0.1$, $\Gamma = 25$, $s = 100$.

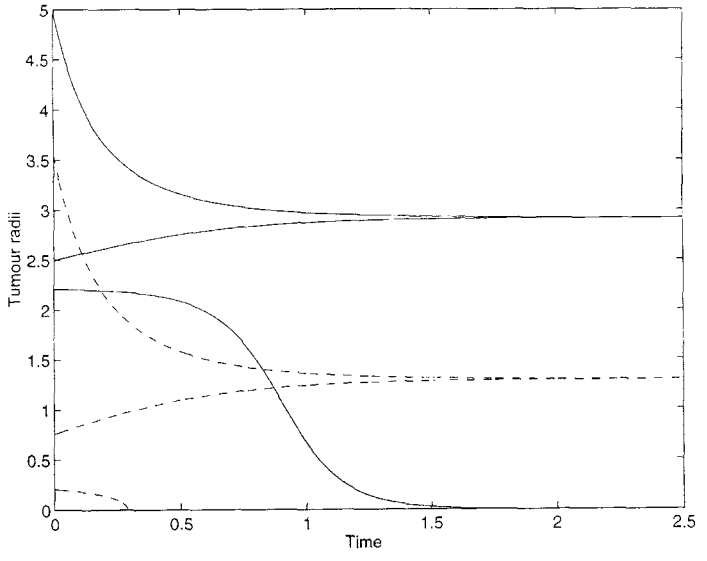

FIGURE 5 Evolution of R and r_{nec} when $S(\sigma) = s\sigma(1 - \sigma/\hat{\sigma})$. If $R(0) < 2.2$ then the tumour decays to zero: otherwise it evolves to a nontrivial, necrotic configuration. Parameter values: $\sigma_\infty = 0.8.\sigma_{\text{nec}} = 0.4$, $\hat{\sigma} = 0.64$, $\lambda = 0.1$, $\Gamma = 25$, $s = 100$.

The effect that the choice of $S(\sigma)$ has on the tumour's growth characteristics becomes apparent when the linear proliferation rate is replaced by a logistic term

$$S(\sigma) = s\sigma\left(1 - \frac{\sigma}{\hat{\sigma}}\right)$$

in (2.2). With $\hat{\sigma}$ constant, we now interpret $s\sigma^2/\hat{\sigma}$ as the cell loss term due to apoptosis. In this case, numerical simulations suggest that two possible outcomes occur: either the tumour decays to zero or it attains a steady, necrotic configuration, the type of behaviour realised depending on the balance between $\hat{\sigma}$ relative to σ_∞ and σ_{nec} (Byrne and

Chaplain, 1996a). For small values of $\hat{\sigma}$ (i.e. strong apoptotic decay) all tumours eventually disappear whereas for larger values of $\hat{\sigma}$ (i.e. weak apoptotic decay) all tumours evolve to a necrotic structure. The simulations suggest that for intermediate values of $\hat{\sigma}$ the steady state is no longer unique and that the limiting behaviour depends on $R(0)$. In such cases, if $R(0)$ is sufficiently small then the tumour still decays to zero whilst larger tumours evolve to necrotic configurations (see Figure 5). The qualitative differences in the steady-state structure of the tumour which arise for the two choices of $S(\sigma)$ remind us how important accurate knowledge of the proliferation rate is for predicting a tumour's growth characteristics.

4 ASYMPTOTIC ANALYSIS

As mentioned above, in real applications the functional forms used to describe expressions such as $N(\sigma)$ and $S(\sigma)$ will be more complicated than those considered in this paper. As such, the model will not, in general, admit explicit analytical solutions. In such cases, most authors present numerical solutions of the model equations. Whilst these are of value, such simulations often obscure the manner in which the different physical processes interact. Insight into the behaviour of the system can be gained by focusing on special cases for which the model equations simplify (Byrne and Chaplain, 1996a). In this section we illustrate how this can be achieved using asymptotic analysis to focus on three special cases which are of practical interest in avascular tumour growth: when the tumour is very small ($0 < R \ll 1$); immediately after the onset of necrosis ($0 < r_{\text{nec}} \ll 1$); and, when the width of the proliferating rim is small ($0 < R - r_{\text{nec}} \ll 1$). The third case is of particular interest since it is frequently observed when MCS are cultured in the laboratory. The same methods can be used to study the effect that different proliferation rates have on the tumour's development. It is also anticipated that the resulting approximate expressions for R and r_{nec} could be used to estimate key parameters from *in vitro* data on MCS. In addition, the approximate, analytical results provide us with some indication of the relative importance of apoptosis and necrosis as cell loss mechanisms at different stages of a tumour's development.

Small Tumour Analysis

When $r_{\text{nec}} = 0$ (3.4) describes the growth rate of the tumour. In the limit as $R \to 0$ this equation reduces to give:

$$\frac{dR}{dt} = \frac{sR}{3}(\sigma_\infty - \tilde{\sigma}) + O(R^3). \tag{4.1}$$

Equation (4.1) shows clearly how the tumour's growth rate depends upon the balance between the rate of cell loss due to apoptosis ($\tilde{\sigma}$) and the rate of cell proliferation which is controlled by the external nutrient concentration (σ_∞). If $\tilde{\sigma} > \sigma_\infty$ the tumour shrinks and we say that the trivial, tumour-free solution ($R = 0$) is stable. As σ_∞ passes through $\tilde{\sigma}$ the stability of the trivial solution changes so that when $\sigma_\infty > \tilde{\sigma}$ the trivial solution is unstable and tumour growth ensues (Byrne and Chaplain, 1995a). As the tumour grows higher order terms become significant and (4.1) ceases to provide an accurate approximation to the tumour's growth rate. In this case we must revert to (3.4).

The Onset of Necrosis

In order to characterise the size of the necrotic core directly after the onset of necrosis we introduce the small parameter ϵ ($0 < \epsilon \ll 1$) and assume that R and r_{nec} can be expressed in terms of ϵ in the following way:

$$R \sim R_0 + \epsilon R_1 + \epsilon^2 R_2 \text{ and } r_{\text{nec}} \sim \epsilon \bar{r}_{\text{nec}}. \tag{4.2}$$

Substituting with (4.2) in (3.1) and equating to zero terms of $O(\epsilon^n)$ the following expressions can be derived:

$$R_0^2 = 6(\sigma_\infty - \sigma_{\text{nec}})/\Gamma = R^{*2}, R_1 = 0,$$
$$R_2 = 3\bar{r}_{\text{nec}}^2/2R_0. \tag{4.3}$$

In (4.3) R^* is the tumour radius at the onset of necrosis, as defined by (3.5).

From (4.3) we deduce that the outer radius of the tumour is almost constant when the necrotic core is small and that variations in $R(t)$ are much smaller than variations in $r_{\text{nec}}(O(\epsilon^2)$ versus $O(\epsilon))$. Using (4.3) and substituting with R and r_{nec} in (3.2) yields an ODE for R_2 which is singular in the limit as $\epsilon \to 0$. To regularise this equation we introduce a short timescale $\tau = t/\epsilon^2$. In terms of τ (3.2) supplies, at leading order,

$$\frac{dR_2}{d\tau} = \frac{sR_0}{15}(3\sigma_\infty - 5\tilde{\sigma} + 2\sigma_{\text{nec}}) \equiv \Lambda, \qquad (4.4)$$

so that the growth rate of the tumour depends upon the balance between cell proliferation, cell loss due to apoptosis and the nutrient concentration at which necrosis is triggered. In particular, the absence in (4.4) of λ leads us to predict that when the necrotic core is small the tumour's growth rate is, to $O(\epsilon^2)$, independent of the rate of cell loss due to necrosis. This result is consistent with results obtained by Eerola *et al.* (1997) who showed that apoptosis is inversely related to necrosis in small cell lung carcinoma.

Integrating (4.4) we obtain the following expressions for R_2 and $\bar{r}_{\text{nec}}$:

$$R_2(\tau) = R_2(\tau = 0) + \Lambda\tau \text{ and } \bar{r}_{\text{nec}} = \left[\frac{2R_0}{3}(R_2(\tau = 0) + \Lambda\tau)\right]^{1/2}.$$

We deduce that if $\Lambda > 0$ then both the tumour and its necrotic core grow whereas if $\Lambda < 0$ then the tumour shrinks and the necrotic core disappears at time $\tau = -R_2(\tau = 0)/\Lambda$. These results link together with those presented in section 3 where R^* was introduced to denote the tumour radius at the onset of necrosis. Given that, for nontrivial solutions, $R_0 = R^* > 0$, we use the definition of Λ (see (3.5) or (4.4)) to make the following prediction which relates the existence of a necrotic core to a specific balance between the system parameters.

- *If* $3\sigma_\infty > 5\tilde{\sigma} - 2\sigma_{\text{nec}}$ *then the tumour will be necrotic when it reaches equilibrium.*

Given estimates of $\sigma_\infty, \sigma_{\text{nec}}$ and $\tilde{\sigma}$ it should be possible to test this claim experimentally. Otherwise, in the absence of complete parameter estimates, the result could be used to construct physical bounds for one of the model parameters. For example, if σ_∞ and σ_{nec} are known and if the tumour possesses a necrotic core at equilibrium we infer that

$$0 \leq \tilde{\sigma} \leq \frac{3\sigma_\infty + 2\sigma_{\text{nec}}}{5}.$$

In this way, we place an upper limit on the rate of cell loss due to apoptosis. The appearance of $\tilde{\sigma}$ and σ_{nec} in the our model prediction leads us to deduce that both necrosis and apoptosis compete on equal footings at this stage of the tumour's development.

That we had to introduce a short timescale in (4.4) to regularise the model equations leads us to make the addition prediction:

- *During the early stages of necrosis the necrotic volume expands rapidly whereas the total tumour volume remains approximately constant.*

This prediction is in good qualitative agreement with independent experimental results obtained by Groebe and Mueller-Klieser (1996). Working with MCS, they observed that the necrotic volume did not grow gradually with spheroid diameter, rather it showed a rapid increase once a few cells had died.

The Thin Proliferating Rim

Introducing the small parameter θ $(0 < \theta \ll 1)$ we assume that, when the proliferating rim is thin, the radius of the necrotic core is related to the outer tumour radius as follows:

$$r_{\text{nec}} = R(1 - \theta r_{n1}) + O(\theta^2).$$

In this case, we derive from (3.1) the following expression which relates the width of the proliferating rim, $\theta R r_{n1}$, to the difference between the external and the necrotic nutrient concentrations:

$$\sigma_\infty - \sigma_{\text{nec}} = \frac{\Gamma}{2}(\theta R r_{n1})^2 = \frac{\Gamma}{2}(R - r_{\text{nec}})^2.$$

From this result we make the following prediction:

- *If the difference between the external nutrient concentration* (σ_∞) *and the nutrient concentration at*

which necrosis occurs (σ_{nec}) *is very small* ($\sigma_\infty - \sigma_{\text{nec}} = O(\theta^2)$) *then at equilibrium the tumour will possess a viable rim of width* $[2(\sigma_\infty - \sigma_{\text{nec}})/\Gamma]^{1/2}$.

This model prediction, which provides us with necessary conditions for obtaining tumours with thin proliferating rims, could be tested experimentally. For example, given estimates of σ_∞, σ_{nec} and Γ we can use this result to estimate the width of the proliferating rim. We remark that our expression for the width of the viable rim agrees with that *assumed* in (Greenspan, 1976). In addition, the result suggests that the proliferating rim tends ultimately to a value which is independent of both time and the rate of cell loss due to apoptosis.

Turning to (3.2), we deduce that R satisfies the following ODE:

$$\frac{1}{s}\frac{dR}{dt} = -\lambda R + \theta(\sigma_{\text{nec}} - \tilde{\sigma})Rr_{n1}$$
$$sim - \lambda R + \theta(\sigma_\infty - \tilde{\sigma})Rr_{n1}.$$

The rate of cell loss due to necrosis is now crucial to the growth rate of the tumour. For example, if $\lambda \sim O(1)$ then the tumour decays exponentially, and necrosis is the dominant cell loss mechanism, with cell proliferation and cell loss due to apoptosis playing secondary roles. However, if $\lambda = \theta\bar{\lambda}$ then the ODE for R reduces to give

$$\frac{1}{s\theta}\frac{dR}{dt} = -\bar{\lambda}R + (\sigma_\infty - \tilde{\sigma})Rr_{n1},$$

so that cell proliferation, cell loss due to apoptosis and necrosis now compete on equal footings. In this case our model analysis leads us to make the following prediction:

- *If the rate of cell loss due to necrosis is small* ($0 < \lambda = \theta\bar{\lambda} \ll 1$), $\sigma_\infty > \tilde{\sigma}$, *and the difference between the external nutrient concentration and the nutrient concentration at which necrosis occurs is also small* ($\sigma_\infty - \sigma_{\text{nec}} = O(\theta^2)$) *then the tumour evolves on a long timescale* $t = O(\theta^{-1})$ *to an equilibrium configuration for which*

$$R = \frac{\sigma_\infty - \tilde{\sigma}}{\theta\bar{\lambda}}\sqrt{\frac{2(\sigma_\infty - \sigma_{\text{nec}})}{\Gamma}} \text{ and } r_{n1} = \frac{\bar{\lambda}}{\sigma_\infty - \tilde{\sigma}}.$$

The predictions in this statement relating to λ, σ_∞, σ_{nec} and Γ need to be tested experimentally. However, the slow evolution of the tumour to its equilibrium configuration agrees with experimental results described by Groebe and Mueller-Klieser (1996).

By linearising about the steady state and inspecting the sign of dR/dt in this neighbourhood it is easy to show that, where it exists, the steady state is stable with respect to time-dependent perturbations (Byrne and Chaplain, 1995a, 1996a).

5 CONCLUSIONS

In this paper we have presented a simple mathematical model that describes the growth of an avascular tumour which contains proliferating and necrotic cells. An external nutrient acts as a source of energy, enabling the cells to proliferate. Necrosis and apoptosis have been introduced as distinct cell loss mechanisms, each responsible for counteracting the proliferative expansion of the tumour. Cell loss due to necrosis describes the death of cells towards the centre of the tumour that results from nutrient deprivation. This mechanism is routinely included in models of avascular tumour growth whereas apoptosis, the second cell loss mechanism, is less commonly included. Apoptosis describes natural cell death and occurs, for example, when a cell exceeds its natural lifespan.

The main aims of the paper were to demonstrate, using numerical and asymptotic techniques, how the relative importance of the two cell loss mechanisms changes as a tumour grows and also generate experimental hypotheses. The numerical simulations furnish us with growth curves showing the evolution of the tumour radius and the necrotic core. By comparing these curves with experimental growth curves, obtained from MCS cultured *in vivo*, it should be possible to test the accuracy of the model. The simulations also enable us to examine how changes in the model parameters effect the tumour's growth characteristics. This is of particular value because it is not always feasible to manipulate individual system parameters in a laboratory.

Since it is often difficult to see how the different physical mechanisms interact when numerical simulations are used, we used asymptotic techniques to study the model equations at three different stages of the tumour's development. In each case the model equations simplified considerably and we were able to determine the relative importance of cell proliferation, cell loss due to necrosis and cell loss due to apoptosis. Most importantly we were able to use our results to generate a number of model predictions, some of which agree with existing data and others which have yet to be validated. For completeness, we repeat the main predictions below:

1. If $\sigma_\infty > \tilde{\sigma}$ then the system can support a non-trivial steady state tumour.
2. At the onset of necrosis the tumour radius is given by $R^* = [6(\sigma_\infty - \sigma_{\text{nec}})/\Gamma]^{1/2}$.
3. During the early stages of necrosis the total tumour volume remains approximately constant whilst the necrotic region expands rapidly.
4. If $3\sigma_\infty > 5\tilde{\sigma} - 2\sigma_{\text{nec}}$ then at equilibrium the tumour possesses a necrotic core.
5. (a) If $0 < \sigma_\infty - \sigma_{\text{nec}} \ll 1$ then at equilibrium the tumour has a thin proliferating rim of width $[2(\sigma_\infty - \sigma_{\text{nec}})/\Gamma]^{1/2}$.
   (b) If, in addition, the rate of cell loss due to necrosis is small and $\sigma_\infty > \tilde{\sigma}$ then the tumour evolves slowly to its equilibrium configuration (which has a thin viable rim).
6. Before the onset of necrosis, during the early stages of a tumour's development, apoptosis is the dominant cell loss mechanism. The appearance of a necrotic core signals an increase in the importance of cell loss due to necrosis and a reduction in the relative importance of cell loss due to apoptosis, this difference becoming more pronounced as the tumour increases in size.

Predictions 1, 2, 4 and 5(a) have yet to be validated by experimental results. However predictions 3 and 5(b) are consistent with results reported by Leith and Michelson (1994) and Groebe and Muller-Klieser (1996). Working with MCS, Groebe and Muller-Klieser observed a rapid increase in the volume of the necrotic region during early necrosis. They also observed a slow decrease in the thickness of the viable rim in large spheroids. Working with clone-A human colon-tumour xenografts, Leith and Michelson (1994) observed that a decrease in the proportion of the tumour containing proliferating cells occurred with the onset of necrosis. In addition, Eerola *et al.* (1997) observed a decrease in the relative importance of apoptosis in small cell lung carcinoma as the tumour developed and the extent of tumour necrosis increased.

In addition to its potential for generating model predictions such as those listed above, one advantage of the asymptotic techniques used in this paper is that they can be applied to other, similar models in which more realistic (nonlinear) expressions are used to describe terms such as cell proliferation, cell loss due to apoptosis and nutrient consumption. This is especially important given the qualitative differences in the steady-state structure of the tumour that can arise when different choices of the cell proliferation rate ($S(\sigma)$) are employed (see Figures 4 and 5).

There are many ways in which our mathematical model could be extended. For example, we could employ more realistic functional forms to describe $S(\sigma)$ and $N(\sigma)$ (Hiltman and Lory, 1983). In addition to nonlinearities, these terms might also include time delays. Such delays reflect the fact that a cell requires a finite amount time to divide. Delays might also be used to describe observed changes in the proliferation and cell loss rates over time (Byrne, 1997a, b; Byrne and Gourley, 1997). For example, it is believed that if the cell proliferation rate gets too large (or too small) then the rate of cell loss due to apoptosis will, after a period of time, adapt to this change by increasing (or decreasing) in magnitude. Another model modification involves relaxing the assumed radial-symmetry of the tumour, and introducing small asymmetric effects to describe tumour invasion or metastasis (Greenspan, 1976; Chaplain, 1993; Byrne and Chaplain, 1996b). If all asymmetric perturbations disappear then we predict that the tumour will grow as a localised, radially-symmetric mass, with no invasion. By contrast, growth of an asymmetric perturbation suggests that the tumour has a propensity for invasion, the growth

rate of the perturbation indicating the degree of aggression.

References

Adam, J. A. (1986) A simplified mathematical model of tumour growth. *Math. Biosci.*, **81**, 229-242.

Adam, J. A. and Maggelakis, S. A. (1990) Diffusion regulated growth characteristics of a spherical prevascular carcinoma. *Bull. Math. Biol.*, **52**, 549-582.

Balding, D. and McElwain, D. L. S. (1985) A mathematical model of tumour-induced capillary growth. *J. Theor. Biol.*, **114**, 53-73.

Byrne, H. M. and Chaplain, M. A. J. (1995a) The growth of non-necrotic tumours in the presence and absence of inhibitors. *Math. Biosci.*, **130**, 151-181.

Byrne, H. M. and Chaplain, M. A. J. (1995b) Mathematical models for tumour angiogenesis: Numerical simulations and nonlinear wave solutions. *Bull. Math. Biol.*, **57**, 461-486.

Byrne, H. M. and Chaplain, M. A. J. (1996a) The growth of necrotic tumours in the presence and absence of inhibitors. *Math. Biosci.*, **135**, 187-216.

Byrne, H. M. and Chaplain, M. A. J. (1996b) The role of cell-cell adhesion in the growth and development of carcinomas. *Math. Comput. Mod.*, **24**, 1-17.

Byrne, H. M. (1997a) The effect of time delays on the dynamics of avascular tumour growth. *Math. Biosci.*, (accepted).

Byrne, H. M. (1997b) Biological inferences from a history-dependent model of avascular tumour growth. (in preparation).

Byrne, H. M. and Gourley, S. A. (1997) The role of growth factors in avascular tumour growth. *Math. Comput. Mod.*, (accepted).

Chaplain, M. A. J. (1993) "The development of a spatial pattern in a model for cancer growth", in *Experimental and Theoretical Advances in Biological Pattern Formation*, (eds. Othmer, H. G., Maini, P. K. and Murray, J. D.), Plenum Press, pp 45-60.

Chaplain, M. A. J. and Britton, N. F. (1993) "On the concentration profile of a growth inhibitory factor in multicell spheroids.", (1993) *Math. Biosci.*, **115**, 233-245.

Chaplain, M. A. J., Benson, D. L. and Maini, P. K. (1994) "Nonlinear diffusion of a growth inhibitory factor in multicell spheroids", (1994) *Math. Biosci.*, **121**, 1-13 (80%).

Chaplain, M. A. J. and Stuart, A. M. (1993) "A model mechanism for the chemotactic response of endothelial cells to tumour angiogenesis factor.", *IMA J. Math. Appl. Med. Biol.*, **10**, 149-168.

Chaplain, M. A. J. (1995) "The mathematical modelling of tumour angiogenesis and invasion" *Acta Biotheor.*, **43**, 387-402.

Darzynkiewicz, Z. (1995) Apoptosis in antitumour strategies — modulations of cell-cycle or differentiation. *J. Cell. Biochem.*, **58**, 151-159.

Dixon, S. C., Soriano, B. J., Lush, R. M., Borner, M. M. and Figg, W. D. (1997) Apoptosis: its role in the development of malignancies and its potential as a novel therapeutic target. *Annals of Pharmacotherapy*, **31**, 76-82.

Durand, R. E. (1990) Multicell spheroids as a model for cell kinetic studies. *Cell Tissue Kinet.*, **23**, 141-159.

Eerola, A. K., Tormanen, U., Rainio, P., Sormunen, R., Bloigu, R., Vahakangas, K., Lehto, V. P., Soini, Y. and Paako, P. (1997) Apoptosis in operated small cell lung carcinoma is inversely related to tumour necrosis and p53 immunoreactivity. *J. Pathol.* **181**, 172-177.

Folkman, J. (1976) The vascularization of tumors. *Sci. Am.*, **234**, 58-73.

Freyer, J. P., Tustanoff, E., Franko, A. J. and Sutherland, R. M. (1984) In situ oxygen consumption rates of cells in V-79 multicellular spheroids during growth. *J. Cell Physiol.*, **118**, 53-61.

Grasl-Kraupp, B., Ruttkay-Nedecky, B., Mullauer, L., Taper, H., Huber, W., Bursch, W. and Schulte-Hermann, R. (1997) Inherent increase of apoptosis in liver tumours: implications for carcinogenesis and tumour regression. *Hepatology*, **25**, 906-912.

Greenspan, H. P. (1972) Models for the growth of a solid tumour by diffusion. *Stud. Appl. Math.*, **52**, 317-340.

Greenspan, H. P. (1976) On the growth and stability of cell cultures and solid tumours. *J. theor. Biol.*, **56**, 229-242.

Groebe, K. and Mueller-Klieser, W. (1991) Distribution of oxygen, nutrient and metabolic waste concentrations in multicellular spheroids and their dependence on spheroid parameters. *Eur. Biophys. J.*, **19**, 169-181.

Groebe, K. and Mueller-Klieser, W. (1996) On the relation between size of necrosis and diameter of tumour-spheroids. *Intl. J. Rad. Oncol. Biol. Phys.*, **34**, 395-401.

Hawkins, N., Lees, J., Hargrave, R., O'Connor, T., Meagher, A. and Ward, R. (1997) Pathological and genetic correlates of apoptosis in the progression of colorectal neoplasia. *Tumour Biology*, **18**, 146-156.

Hickman, J. A., Potten, C. S., Merritt, A. J. and Fisher, T. C. (1994) Apoptosis and cancer chemotherapy. *Phil. Trans. Roy. Soc. Lond. B.*, **345**, 319-325.

Hiltman, P. and Lory, P. (1983) On oxygen diffusion in a spherical cell with Michaelis-Menten oxygen uptake kinetics. *Bullet. Math. Biol.*, **45**, 661-664.

Kane, D. J., Ord, T., Anton, R. and Bredesen, D. E. (1995) Expression of bcl-2 inhibits necrotic neural cell death. *J. Neurosci. Res.*, **40**, 269-275.

Kastan, M. B., Canman, C. E. and Leonard, C. J. (1995) P53, cell cycle control and apoptosis: implications for cancer. *Cancer and Metastasis Reviews*, **14**, 3-15.

Kerr, J. F. R. (1971) Shrinkage necrosis: a distinct mode of cellular death. *J. Path.*, **105**, 13-20.

Kerr, J. F. R., Wylie, A. H. and Currie, A. R. (1972) Apoptosis: a basic biological phenomenon with wide-ranging implications in tissue-kinetics. *Br. J. Cancer*, **29**, 239-257.

Kerr, J. F. R., Winterford, C. M. and Harmon, B. V. (1994) Apoptosis — its significance in cancer and cancer therapy. *Cancer*, **73**, 2013-2026.

Kiberu, S. W., Pringle, J. H., Sobolewski, S., Murphy, P. and Lauder, I. (1996) Correlation between apoptosis, proliferation and bcl-2 expression in malignant non-Hodgkins-lymphoma. *J. Clin. Pathol.*, **49**, M268-M272.

Kressel, M. and Groscurth, P. (1994). Distinction of apoptotic and necrotic cell-death by in-situ labelling of fragmented DNA. *Cell Tiss. Res.*, **278**, 549-556.

Landry, J., Freyer, J. P. and Sutherland, A. M. (1982) A model for the growth of multicell spheroids. *Cell Tissue Kinet.*, **15**, 585-594.

Leith, J. T. and Michelson, S. (1994) Changes in the extends of viable and necrotic tissue, interstitial fluid pressure, and proliferation kinetics in clone-A human colon-tumour xenografts as a function of tumour size. *Cell Prolif.*, **27**, 723-739.

McElwain, D. L. S. and Morris, L. E. (1978) Apoptosis as a volume loss mechanism in mathematical models of solid tumour growth. *Math. Biosci.*, **39**, 147-157.

Merritt, A. J., Potten, C. S., Watson, A. J. M., Loh, D. Y., Nakayama, K. and Hickman, J. A. (1995) Differential expression

of BCL-2 in intestinal epithelia — correlation with attenuation of apoptosis in colonic crypts and the incidence of colonic neoplasia. *J. Cell Sci.*, **108**, 2261-2271.

Muthukkaruppan, V. R., Kubai, L. and Auerbach, R. (1982) Tumor-induced neovascularization in the mouse eye. *J. Natn. Cancer Inst.*, **69**, 699-705.

Mueller-Klieser, W. (1987) Multicellular spheroids: a review on cellular aggregates in cancer research. *J. Cancer Res. Clin. Oncol.*, **113**, 101-122.

Orme, M. E. and Chaplain, M. A. J. (1996) A mathematical model of vascular tumour growth and invasion. *Math. Comput. Modelling*, **23**, 43-60.

Potten, C. S. (1992) The significance of spontaneous and induced apoptosis in the gastrointestinal tract of mice. *Cancer Met. Rev.*, **11**, 179-195.

Rowan, S. and Fisher, S. E. (1997) Mechanisms of apoptotic cell death. *Leukaemia*, **11**, 457-465.

Shao, Z. M., Jiang, M., Wu, J., Yu, L. M., Han, Q. X., Zhang, T. Q. and Shen, Z. Z. (1996) Inhibition of apoptosis in human breast cancer as related to prognosis. *Oncol. Rep.*, **3**, 1183-1186.

Sutherland, R. M. and Durand, R. E. (1984) Growth and cellular characteristics of multicell spheroids. *Recent Results in Cancer Research*, **240**, 177-184.

Thames, H. D., Ruifrok, A. C. C., Milas, L., Hunter, N., Mason, K. A., Terry, N. H. A. and White, R. A. (1996) Accelerated repopulations during fractionated-irradiation of a murine ovarian-carcinoma — down-regulation of apoptosis as a possible mechanism. *Intl. J. Rad. Oncol. Biol. Phys.*, **35**, 951-962.

Tu, H. C., Jacobs, S. C., Borkowski, A. and Kyprianou, N. (1996) Incidence of apoptosis and cell-proliferation in prostate-cancer — relationship with TGF-beta(1) and bcl-2 expression. *Intl. J. Cancer*, **69**, 357-363.

Tubiana, M. (1971) The kinetics of tumour cell proliferation and radiotherapy. *Br. J. Radiol.*, **44**, 325-347.

Ward, J. P. and King, J. R. (1997) Mathematical modelling of a vascular-tumour growth. IMA J. Math. Appl. Med. Biol., **14**, 39-69.

Watson, A. J. M., Merritt, A. J., Jones, L. S., Askew, J. N., Anderson, E., Becciolini, A., Balzi, M., Potten, C. S. and Hickman, J. A. (1996) Evidence for reciprocity of BCL-2 and P53 expression in human colorectal adenomas and carcinomas. *Br. Jl. Cancer*, **73**, 889-89.